DR RICCARDO RONZONI (Orcid ID : 0000-0002-3981-8104)
DR ANNAMARIA FRA (Orcid ID : 0000-0002-4327-3004)
DR ELENA MIRANDA (Orcid ID : 0000-0002-0586-8795)
DR JAMES A IRVING (Orcid ID : 0000-0003-3204-6356)

Received Date : 22-Jun-2020
Revised Date : 28-Aug-2020
Accepted Date : 12-Oct-2020

Supinfo: 2 Fig

Color: Fig 1-5

The molecular species responsible for α_1-antitrypsin deficiency are suppressed by a small molecule chaperone

Riccardo Ronzoni[1], Nina Heyer-Chauhan[1], Annamaria Fra[2], Andrew C. Pearce[3], Martin Rüdiger[3], Elena Miranda[4], James A. Irving[1]* and David A. Lomas[1]*

[1]UCL Respiratory, Division of Medicine, Rayne Building, University College London, London, WC1E 6JF, UK.

[2]Department of Molecular and Translational Medicine, University of Brescia, 25123 Brescia, Italy.

[3]GSK Medicines Research Centre, Gunnels Wood Rd, Stevenage, SG1 2NY, UK.

[4]Department of Biology and Biotechnologies 'Charles Darwin' and Pasteur Institute – Cenci-Bolognetti Foundation, Sapienza University of Rome, Italy.

*Equal senior authors.

Address for correspondence: Dr Riccardo Ronzoni, UCL Respiratory, Rayne Institute, University College London, London. WC1E 6JF E-mail: r.ronzoni@ucl.ac.uk Tel.: +44 (0)2031087735

Running Title: Preventing intracellular polymerisation of Z α1-antitrypsin

Abbreviations:

BafA1, Bafilomycin A1; ConA, Concanavalin A; DMSO, Dimethyl sulfoxide; ELISA, Enzyme-Linked Immunosorbent Assay; Endo H, endoglycosidase H; ER, Endoplasmic Reticulum; IP, immunoprecipitation; iPSCs, Induced pluripotent stem cells; mAb, monoclonal antibodies; NP-40, Nonidet P40; PAS, Periodic Acid-Schiff; PNGase F, peptide-N-glycosidase F; Tet-On, Tetracycline-controlled transcriptional activation.

Key words: α_1-antitrypsin, polymerisation, folding intermediate, polymer inhibitor, secretion.

Conflict of Interest: David Lomas is an inventor on patent PCT/GB2019/051761 that includes the small molecule inhibitor of polymerisation c716. The intellectual property has been transferred from GlaxoSmithKline to UCL Business who have licenced it to a third party.

Abstract

The formation of ordered Z (Glu342Lys) α_1-antitrypsin polymers in hepatocytes is central to liver disease in α_1-antitrypsin deficiency. *In vitro* experiments have identified an intermediate conformational state (M*) that precedes polymer formation but this has yet to be identified *in vivo*. Moreover, the mechanism of polymer formation and their fate in cells have been incompletely characterised. We have used cell models of disease in conjunction with conformation-selective monoclonal antibodies and a small molecule inhibitor of polymerization to define the dynamics of polymer formation, accumulation and secretion. Pulse-chase experiments demonstrate that Z α_1-antitrypsin accumulates as short chain polymers that partition with soluble cellular components and are partially secreted by cells. These precede the formation of larger, insoluble polymers with a longer half-life (10.9 +/- 1.7 h and 20.9 +/ 7.4 h for soluble and insoluble polymers respectively). The M* intermediate (or a byproduct thereof) was identified in the cells by a conformation-specific monoclonal antibody. This was completely abrogated by treatment with the small molecule which also blocked the formation of intracellular polymers. These data allow us to conclude that: the M* conformation is central to polymerization of Z α_1-antitrypsin *in vivo*; preventing its accumulation represents a tractable approach for pharmacological treatment of this condition; polymers are partially secreted; and polymers exist as two distinct populations in cells whose different dynamics have likely consequences for the aetiology of the disease.

Introduction

α_1-Antitrypsin is the archetypal member of the serpin superfamily of proteins and a major inhibitor of neutrophil elastase in humans [1]. Plasma deficiency of this protease inhibitor predisposes to early-onset panlobular basal emphysema due to de-regulated elastase activity within the lung [2]. The common severe Z deficiency variant of α_1-antitrypsin (Glu342Lys) results in the formation of long-chains of ordered aggregates termed polymers. These polymers accumulate within the endoplasmic reticulum (ER) of hepatocytes, condensing as periodic acid-Schiff (PAS) positive inclusions [1–5] that are associated with neonatal hepatitis, cirrhosis and hepatocellular carcinoma [6].

In vitro studies demonstrated that the Glu342Lys substitution perturbs folding of Z α_1-antitrypsin allowing the formation of a monomeric unstable intermediate, denoted M* [7]. This state is associated with changes in β-sheet A and helix F [3,7–10] and is a precursor to oligomerisation involving an intermolecular domain-swap [3,11,12]. Serpin polymerisation is a form of non-amyloid aggregation. The process involves β-sheet interactions but is distinguished by an intermediate that remains largely well-folded [13] with the subunits of the resulting polymers exhibiting only minimal structural perturbation with respect to the native conformation [11,12,14–16]. These ordered structures most likely explain the failure of polymers to activate the unfolded protein response in cellular and animal models of the disease [17,18]. However, the accumulation of α_1-antitrypsin polymers within hepatocytes results in an increase in ER volume, increased intraluminal viscosity [19] and the formation of ER-derived membrane-bound inclusions [20]. Moreover, the extent of accumulation of Z α_1-antitrypsin and the associated hepatotoxicity depends on the efficiency of both ER-associated degradation (ERAD) [21–24] and lysosomal-associated degradative pathways [25–27].

The structural variability of α_1-antitrypsin has resulted in the development of a toolkit of conformation-specific monoclonal antibodies (mAb) that are able to recognise different conformations of this protein. The polymer-specific 2C1 mAb [28,29] that recognises intrahepatic α_1-antitrypsin polymers revealed that polymers of α_1-antitrypsin are present in the circulation of all individuals with Z α_1-antitrypsin deficiency [30]. The origin of these polymers is unclear but our

recent data from cell models of disease demonstrated indirectly that polymers can be secreted by cells [31]. The 5E3 mAb was used to characterize the polymerisation-prone intermediate M* [32] *in vitro*, but has not been evaluated in a cellular model of α_1-antitrypsin deficiency.

We have used metabolic labelling and antibodies with different conformational preference (Table 1) to characterise the kinetics of polymer formation and resolution and the intracellular distribution and secretion of Z α_1-antitrypsin polymers in cellular models of disease.

Results

Intracellular Z α_1-antitrypsin polymers partition in both the NP-40-soluble and -insoluble fractions

A previously established and validated inducible Tet-On cellular system [19] was used to investigate the partitioning of intracellular polymers of Z α_1-antitrypsin. CHO K1 cells expressing Z or wild-type M α_1-antitrypsin were induced with 0.5 μg/mL doxycycline for 48 h and lysed in a buffer containing 1% v/v NP-40. Centrifugation at 12,000 g was used to separate the soluble from the insoluble fraction, the latter was then mechanically resuspended in lysis buffer and sonicated. Biochemical analysis of these fractions and the culture medium supernatants by denaturing SDS-PAGE and immunoblot confirmed that M α_1-antitrypsin was only present in the cellular soluble and secreted fractions (Fig. 1A, upper panel and graph); the wild-type variant is known to efficiently transit through the secretory pathway to the extracellular medium [19,33,34]. In contrast, Z α_1-antitrypsin accumulated in both the NP-40 soluble and insoluble fractions and was present at lower level in the cell medium compared to M α_1-antitrypsin (Fig. 1A, lower panel and graph).

The NP-40 soluble and insoluble fractions were then analysed by non-denaturing PAGE and immunoblot for total α_1-antitrypsin (Fig. 1B). The soluble fraction obtained from cells expressing M α_1-antitrypsin migrated as a single monomeric band, whilst the soluble fraction from cells expressing Z α_1-antitrypsin showed a ladder of higher molecular weight forms consistent with a population of α_1-antitrypsin polymers of variable size [4]. Of note, the broad profile of the soluble fraction exhibited an overall faster migration (Fig. 1B, *lower*) and contained distinct bands that matched, allowing for differences in N-glycosylation maturation states, with corresponding bands in the supernatant. The insoluble fraction, instead, was characterised by a high molecular weight-shifted smear and the absence of low molecular weight bands. A fraction of this sample was trapped in the stacking gel suggesting the additional presence of larger, higher molecular weight species.

The presence of α_1-antitrypsin monomers and polymers in the soluble and insoluble intracellular fractions was analysed by sequential immunoprecipitation (IP) using antibodies with differential

conformational selectivity (Table 1 and Fig. 1C). First, polymers were immunoprecipitated three times with the anti-polymer 2C1 mAb [28] and then residual monomer captured in one round with the non-conformation-selective 3C11 mAb [30], using the supernatant of each IP as the input for the next one (Fig. 1C, *SET 1*). Cells expressing M α_1-antitrypsin showed a single band positive for 3C11 in the soluble fraction and no 2C1 recognition in either cellular fraction, confirming its monomeric state under the expression conditions used. The soluble fraction from cells expressing Z α_1-antitrypsin was positive for 2C1 and Z α_1-antitrypsin could still be immunoprecipitated with 3C11 after three rounds of polymer depletion. In contrast, three rounds of immunoprecipitation of the insoluble fraction with 2C1 depleted virtually all α_1-antitrypsin, with no residual non-polymeric material recognised by the 3C11 mAb. In a control experiment the order of the mAbs was reversed (three rounds with 3C11 and a final one with 2C1). As expected, all α_1-antitrypsin was immunoprecipitated by the non-conformation-selective 3C11 mAb (Fig. 1C, *SET 2*).

Z α_1-antitrypsin polymers are secreted through the canonical secretory pathway

Radiolabeling-based approaches provide a means to follow the molecular fate of a protein in a dynamic system without the perturbations that may be introduced by fluorescent tags. We investigated the kinetics of formation and accumulation of α_1-antitrypsin polymers by pulse-chase experiments. CHO K1 cells expressing M or Z α_1-antitrypsin were pulse-labeled for 10 minutes with ^{35}S-methionine and cysteine and, at the chase times indicated in Figure 2A, the culture medium was collected and the cells lysed in NP-40 buffer. M α_1-antitrypsin samples were immunoprecipitated with 3C11 mAb to recover all α_1-antitrypsin (monomeric, as demonstrated in Fig. 1, Fig. 2A, *top panels*, and Fig. 2B, *left panel*), while the Z α_1-antitrypsin samples were sequentially immunoprecipitated with the 2C1 anti-polymer mAb (Fig. 2A, *middle panels* and Fig. 2B, *Z - polymers*) and then with the 3C11 mAb (Fig. 2A, *lower panels* and Fig. 2B, *Z - monomers*).

As shown in Figs. 2A and 2B, in cells expressing the Z variant, radiolabelled monomeric α_1-antitrypsin was detectable at the initial 0 h time point but intracellular soluble polymers only became visible after a delay of 2 h and gradually increased to plateau at 8 h. Soluble extracellular polymers became detectable after 4 h of chase. In the insoluble fraction, polymers were apparent from the 8 h

time point and also increased with time, without exhibiting a plateau over the duration of the experiment.

In the autoradiographs (Fig. 2A) the secreted material (both monomeric and polymeric Z α_1-antitrypsin, white arrowheads) had a higher molecular mass compared to the intracellular species (black arrowheads), as is characteristic of mature glycoproteins secreted through the canonical secretory pathway [28,31]. Analysis of the N-linked glycosylation state was performed to assess the type of glycans present in the extracellular polymers. Polymers immunoprecipitated by 2C1 mAb from culture media of Z α_1-antitrypsin cells pulsed as in Figure 2A were subjected to digestion with peptide-N-glycosidase F (PNGase F), which removes all types of N-linked glycans, or endoglycosidase H (endo H), which cleaves pre-Golgi glycans only. All secreted α_1-antitrypsin was sensitive to digestion by PNGase F but resistant to treatment with endo H (Fig. 2C). This demonstrated that at all time-points only mature glycans were present in extracellular polymers and therefore that their presence in the media was the result of passage through the secretory pathway and not a cell lysis-related artefact.

Insoluble Z α_1-antitrypsin polymers have a longer intracellular half-life than soluble polymers

Soluble Z α_1-antitrypsin polymers reached a peak at approximately 4 h and remained stable until 12 h, while insoluble polymers were still increasing after 12 h of chase (Fig. 2A). The kinetics of clearance of these polymers was assessed with a long metabolic labeling experiment. CHO K1 cells expressing Z α_1-antitrypsin were metabolically labeled with ^{35}S methionine and cysteine for 24 h. At the end of the labeling time, the radioactive culture medium was replaced with normal medium and the cells were grown for a further 12 h. This prolonged 'conversion time', was designed to promote the incorporation of all the radioactive monomeric Z α_1-antitrypsin molecules into polymers. Following the conversion period, cells were chased for up to 72 h and polymeric α_1-antitrypsin was immunoprecipitated with the 2C1 mAb (Fig. 2D). This analysis demonstrated that soluble polymers were cleared more rapidly from cells than the insoluble counterpart. The half-time for the clearance of intracellular soluble polymers was 10.9 +/- 1.7 h, while the half-time for the insoluble polymers was

20.9 +/ 7.4 h (Table 2). It is notable that while soluble polymers were almost entirely cleared following the 72h chase, a residual insoluble component remained.

In order to verify the data obtained in the inducible CHO K1 cell lines and to expand our analysis to a more physiologically relevant context, the same approach was applied to induced pluripotent stem cell (iPSC)-derived hepatocytes. These had been generated previously using fibroblasts from an individual homozygous for the Z variant of α_1-antitrypsin [35,36]. iPSC-derived hepatocytes pre-differentiated for 23 days were revived from frozen stocks and kept in specific medium and under hypoxic conditions in order to promote further hepatic differentiation [37]. At day 35 post-differentiation, cells were starved, radioactively labeled with ^{35}S methionine and cysteine for 24 h and incubated for 12 h in non-radioactive medium to allow the conversion of radioactive α_1-antitrypsin monomers into polymers. Culture media were collected and cells processed every 12 h up to 108 h post-pulse. Intracellular soluble and insoluble fractions of α_1-antitrypsin polymers were immunoprecipitated with the 2C1 mAb and analysed as above. In this cell system soluble polymers also exhibited a shorter half-time 14.6 +/- 6.2 h compared with 19.1 +/- 4.9 h for insoluble polymers (Table 2).

Circulating polymers of Z α_1-antitrypsin have a predominantly intracellular origin

Our data provide direct evidence that polymers are actively secreted by cells. This has potential implications for the interpretation of polymers identified in patient plasma [30]. However, while plasma contains a complex mixture of molecules, including sugars and proteins such as serum albumin which are known to act as stabilisers against denaturation [38], it is unknown whether polymers can form spontaneously in the circulation. A previous experiment in which plasma samples from Z α_1-antitrypsin homozygotes were incubated *in vitro* at 37°C for 3 days showed no increase in polymer content [30]. To extend this study, plasma samples from three different Z α_1-antitrypsin homozygote individuals were incubated at 20°C, 37°C, 41°C, 45°C and 50°C for 24 h and polymer formation was assessed by ELISA with the 2C1 mAb relative to recognition of the total α_1-antitrypsin population by the 3C11 mAb (Fig. 3A, first bar). There was no significant increase in the α_1-antitrypsin polymer signal following 24 h incubation over this range of temperatures (Fig. 3A, bars 3 to 7). Plasma samples from the same patients were also incubated at 37°C for 1, 3 and 10 days,

representing 0.2-, 0.6- and 2-fold the half-life of Z α_1-antitrypsin in the circulation [39], and analysed again by 2C1 mAb ELISA. Again, no significant difference in polymer signal was observed after 3 and 10 days of incubation (Fig. 3B).

The plasma samples were also concentrated by concanavalin A pull-down and analysed on a non-denaturing gel followed by western blot with the 2C1 mAb (Fig. S1). This analysis showed a small but non-significant increase in polymer content after 10 days. Together, these data support the conclusion that Z α_1-antitrypsin has marked stability in plasma and accordingly the primary source of circulating polymer is most likely secretion from cells.

Soluble and insoluble polymers are cleared by different mechanisms of degradation

ER-associated degradation, mediated by the proteasome, has previously been identified as the major contributor to turnover of the Z α_1-antitrypsin variant [9,22,40–43]. CHO K1 cells expressing Z α_1-antitrypsin were subjected to pulse chase in the presence of the reversible inhibitor MG132 in order to investigate the effect of proteasomal degradation on the kinetics of accumulation and secretion of the polymer populations. Treatment with the inhibitor, compared to the kinetics of untreated cells shown in Fig. 2 (and reported in Fig. 4, *lower panel*, NT), resulted in increased accumulation of polymers in the soluble but not in the insoluble intracellular fractions, and increased polymeric and total α_1-antitrypsin in the culture medium (Fig. 4A, *upper panel* and Fig. 4B, *upper panels*). MG132 did not appreciably alter the accumulation of monomer in the supernatant over time, but instead led to the intracellular retention of a monomeric component (Fig. 4B, *lower panels*).

Recent work has shown that in addition to an autophagy-mediated mechanism [43], Z α_1-antitrypsin polymers are degraded via a distinct lysosome-associated system [27]. We thus evaluated the clearance of soluble and insoluble intracellular polymers by lysosomes in our cell model. CHO K1 cells expressing Z α_1-antitrypsin were induced with doxycycline for 48 h, labelled for 15 minutes with ^{35}S methionine and cysteine and then treated for 16 h with either 50 nM Bafilomycin A1 (BafA1), a drug capable of inhibiting the lytic activity of lysosomes, or with a DMSO control. Cells were processed at different time points as shown in Fig. 4C and intracellular fractions were immunoprecipitated first with the 2C1 mAb for polymers and then with the 3C11 mAb for residual

non-polymeric α_1-antitrypsin. Treatment with BafA1 caused a small but non-significant increase in the quantity of insoluble polymers but had no effect on soluble polymers or monomeric Z α_1-antitrypsin.

An experimental compound, c716, prevents intracellular polymer formation and increases secretion

We have developed a small molecule inhibitor of polymerisation, c716, that is active *in vivo* and that prevents the formation of M* *in vitro* [44]. To investigate its behavior under the experimental conditions considered here, CHO K1 cells were seeded in the presence of DMSO or c716 and subsequently induced to produce Z α_1-antitrypsin for 48 h before being starved, pulsed and processed as described in Fig 1. Intra- and extracellular Z α_1-antitrypsin were sequentially immunoprecipitated with 2C1 and 3C11 mAbs. The experimental compound abolished the formation of both soluble and insoluble polymers (Fig. 5A, *upper panels and graphs*) and increased the secretion of Z α_1-antitrypsin (Fig. 5A, *lower right panel and graphs*). Indeed, treatment with the compound resulted in rates of secretion similar to those of the wild-type M α_1-antitrypsin (compare Fig. 5A, *right graph* with Fig. 2B, *left graph*), increasing the amount secreted after 1 h by ~5-fold from 5.2 ± 0.2 % (±SD, n=2) to 28.0 ± 5.3 % (±SD, n=2).

The monomeric intermediate M* is the key species for Z α_1-antitrypsin intracellular polymer formation

In vitro experiments have shown that α_1-antitrypsin folds *via* an intermediate ensemble [43] before reaching its native monomeric state [13,45,46]. Folding is rapid for wild-type M α_1-antitrypsin but is delayed for the Z mutant, increasing the population of these intermediate conformations [47]. One of these conformations, that we have termed M*, is a precursor to polymer formation and elongation [3,7,48,49]. This molecular species, or a monomeric byproduct thereof, is sufficiently persistent to be detectable *in vitro* [46,49,50] and is recognised by the 5E3 mAb [32] (Table 1). The presence of M* in a cellular environment has not been established; we therefore made use of the 5E3 mAb and c716 to determine its role in intracellular polymer formation.

CHO K1 cells expressing Z α_1-antitrypsin were induced with doxycycline and treated for 8 h with DMSO, c716, or MG132. Intra- and extracellular fractions were collected and subjected to sequential immunoprecipitations, first with the 2C1 anti-polymer mAb (four rounds to guarantee complete depletion, Fig. S2), once with the anti-M* 5E3 mAb and finally with the 3C11 anti-total α_1-antitrypsin mAb. 2C1-positive polymers were efficiently immunoprecipitated from the NP-40 soluble intracellular fraction (Fig. 5B, *left panels*). However, a fraction remained that was immunoprecipitated by the 5E3 mAb and a residual amount of α_1-antitrypsin that was immunoprecipitated by the 3C11 mAb, corresponding to the native monomer. Inhibition of ERAD with the proteasomal inhibitor MG132 slightly increased the quantity of polymers recognised by 2C1 mAb with a corresponding decrease in monomers detected by the 3C11 mAb.

The extracellular fraction was characterised by the presence of polymers and native folded monomers (Fig.5B, *right panel*, NT lanes); treatment with MG132 increased the secretion of α_1-antitrypsin polymers and decreased the accumulation of monomer (Fig. 5B, *right panel*, MG132 lanes). It is interesting to note that little extracellular material could be immunoprecipitated by 5E3 mAb, demonstrating the intracellular nature of this folding intermediate and the specificity of the mAb. Stabilisation of a native-like state using c716 reduced the formation of M* and polymers, favouring the secretion of the monomeric form of Z α_1-antitrypsin (Fig. 5B, *right panel*). The level of insoluble polymers remained unchanged upon treatment with MG132 while treatment with c716 completely abolished the presence of polymers and M* in this fraction (Fig. 5A).

Discussion

The Z (Glu342Lys) mutant of α_1-antitrypsin misfolds and forms linear unbranched polymer chains in the ER. It has been shown in cell models of disease that proteostatic degradative mechanisms – ERAD, autophagy and lysosomal-associated degradation – compensate to some degree for this intracellular burden of misfolded and aggregated protein [18,21,22,27,42,43]. However, a hallmark of α_1-antitrypsin deficiency is the deposition of polymers of mutant α_1-antitrypsin as PAS positive inclusions within hepatocytes [3]. The processes that result in this retention of α_1-antitrypsin are incompletely characterised.

Polymers of α_1-antitrypsin partition into components of cellular extracts that can be defined as 'NP-40-soluble' and 'NP-40 insoluble' [42,51], but it has not been determined whether these reflect a single population of molecules or two populations with distinct characteristics. Here we investigated in detail the kinetics of formation, deposition and secretion of Z α_1-antitrypsin polymers. Our data show that the two populations of polymers with differential solubility do indeed exhibit different characteristics: the NP-40 soluble fraction contained a mixture of monomers and lower-molecular weight polymers, with a shorter cellular half-life and whose levels increased in the presence of the proteasomal inhibitor MG132. In contrast, the NP-40 insoluble fraction lacked monomers, had a generally larger polymer size distribution, exhibited a longer half-life and was unaffected by MG132. Notably, the latter population appeared to include a component that was not degraded by the cellular proteostatic mechanisms over the course of a 72 hours experiment. We speculate that this may represent the species that form intractable inclusions within the liver of Z α_1-antitrypsin individuals. A limited subset of polymers appeared in the culture medium at a similar rate to their appearance in the intracellular soluble fraction and with a similar size profile, suggesting progression from formation to secretion. These extracellular polymers were sensitive to PNGase F but resistant to endo H digestion, in keeping with the maturation of N-glycans during transit through the Golgi complex along the canonical secretory pathway [52]. Additionally, the faster migration of the bands under electrophoresis of the soluble fraction from 4 h onwards is consistent with trimming of N-glycans that occurs in the ER or in the cis-Golgi [53].

These modifications were not seen in insoluble polymers, suggesting that they are inaccessible to the enzymes that process N-glycans. Treatment with the proteasome inhibitor MG132 increased the formation of intracellular soluble and secreted polymers but had no effect on insoluble intracellular polymers. This supports the hypothesis that while soluble polymers are trafficked through the secretory pathway and into the extracellular space, insoluble polymers represent a molecular endpoint that cannot be resolved by proteasomal degradation but that must be resolved by alternative cellular homeostatic processes such as autophagy.

The CHO cell model faithfully recapitulates the handling of mutant variants of α_1-antitrypsin seen in other cellular models [23,54], with the benefits of inducible and titratable expression and robust characteristics in cell culture. We confirmed our findings using an iPSC model of Z α_1-antitrypsin deficiency [35,36], which showed similar half-times for the clearance of soluble and insoluble polymers. In both cellular models, a longer turnover time for insoluble polymers, together with the differing effect of proteasomal inhibition on polymer pools, suggests that soluble and insoluble polymers are handled in different ways; smaller and more soluble polymers can be secreted, whereas larger ones, which we hypothesise represent the precursors of the inclusion bodies seen in pathological specimens, are more persistent and only partially degraded by an alternative pathway related to lysosomal degradation [43,55].

We have shown previously that polymers of α_1-antitrypsin can be detected in the circulation of all subjects who carry a Z allele [56]. Our observation that polymers of Z α_1-antitrypsin can be secreted by cells *in vitro*, coupled with the inability to induce polymer formation in plasma samples incubated at either high temperature or for prolonged times, allows us to conclude that the polymers found in circulation are most likely the result of secretion of soluble polymers from hepatocytes. Circulating polymer levels therefore represent a potential 'window' into the efficacy of the proteostatic processes that regulate the formation and accumulation of α_1-antitrypsin polymers in the liver of individuals with α_1-antitrypsin deficiency.

Many *in vitro* studies have established that α_1-antitrypsin folds via an intermediate ensemble [13,27,32,57] that samples a polymerisation-prone intermediate state that we have termed M* [3,7,13,33,47,49,50]. However, the presence of M* within the ER as an intermediate on the Z α_1-antitrypsin secretion pathway has not been established. Using the 5E3 mAb that detects M* [43] and a small molecule that stabilises α_1-antitrypsin against M* formation, we identified three different conformational species within the NP-40 soluble fraction in cells expressing Z α_1-antitrypsin: α_1-antitrypsin polymers, the M* intermediate and a residual conformer that is most likely native monomer. Using MG132, the M* population was found to be unaffected by the ERAD pathway, indicating that this molecular state is either not recognised as aberrant or is assimilated sufficiently rapidly into polymers to evade degradation. In contrast, the formation of M* was suppressed almost completely by c716, resulting in an increase in native monomer and inhibition of both soluble and insoluble polymer formation. Thus, both soluble and insoluble species have a common origin and are not formed by alternative pathways. The compound also restored the secretion profile of Z α_1-antitrypsin to that of the wild-type protein [19,34], demonstrating that M* is a key point in the process of Z α_1-antitrypsin folding, degradation and polymerisation within the ER of cells.

In summary, our data allow us to propose a model for the handling of Z α_1-antitrypsin within the ER. The nascent α_1-antitrypsin polypeptide folds *via* M* to native monomer to become incorporated into a polymer in the soluble fraction of the cell. This polymer can in turn become insoluble through mechanisms that have yet to be elucidated, can be secreted, or be degraded. As these secreted polymers are a product of the intracellular processes of expression, M* formation, oligomerisation, soluble-insoluble partition and secretion, they potentially represent a useful reporter of intrahepatic polymerisation for polymer-blocking therapies in individuals with α_1-antitrypsin deficiency.

Materials and Methods

Inducible cell lines and iPSC-derived hepatocytes

Chinese hamster ovary (CHO K1) cell lines expressing M or Z α_1-antitrypsin under the tetracycline-inducible promoter [19] were maintained in Dulbecco's modified Eagle's medium (DMEM) supplemented with 10% v/v tetracycline-free fetal bovine serum (Takara Bio, Saint-Germain-en-Layne, France), 1% w/v penicillin/streptomycin, 200 μg/mL geneticin, and 500 μg/mL hygromycin B (both selective antibiotics from Invitrogen, Carlsbad, CA) at 37ºC and 5% v/v CO_2. Before each experiment, cells were seeded at a density of $16.3x10^4$ cells/cm^2 and induced to express α_1-antitrypsin with 0.5 μg/mL doxycycline for 48 h.

iPSC-derived hepatocytes and supplements for cell media were supplied by DefiniGEN (DefiniGEN Ltd, Cambridge, UK). Cells were revived and maintained as advised by the supplier. Cells were differentiated in mature hepatocytes after 10 days of culture in hypoxic conditions (5% v/v CO_2, 5% v/v O_2, 90% v/v N_2) in their recommended supplemented medium.

Cell lysis, polymer extraction and immunoprecipitation

Both CHO K1 cells and iPSC-derived hepatocytes were lysed at a concentration of $2.5x10^6$ cells/mL in 1% v/v NP-40 buffer (10 mM Tris pH 7.4, 300 mM NaCl, 1% v/v NP-40) supplemented with protease inhibitors (Roche Ltd, Hertforshire, UK). Cell lysates were collected and mixed for 30 min at 4ºC on a rotator mixer. 1% v/v NP-40-insoluble and -soluble fractions were separated by centrifugation at 16,000 g for 15 min at 4ºC. The supernatant was collected (1% v/v NP-40 soluble fraction), while the pellet (1% v/v NP-40 insoluble fraction) was washed twice in 1% v/v NP-40 buffer and mechanically resuspended in an equal volume of 1% v/v NP-40 buffer supplemented with protease inhibitors. The 1% v/v NP-40 insoluble fraction was finally solubilized by sonication at 1.15KHz (5μm amplitude) for 15 sec at RT (Soniprep150, MSE Ltd, London UK).

For analysis in non-denaturing PAGE (polyacrylamide gel electrophoresis), total α_1-antitrypsin from cell lysates and culture medium samples was concentrated using concanavalin A (ConA)-conjugated

agarose beads (Sigma Aldrich Co, Dorset UK). Samples were diluted 1:2 with binding buffer (20 mM Tris pH7.0, 0.5 M NaCl) and incubated overnight on the rotator at 4ºC. Elution was performed by incubating the beads with 1 M methyl-α-D-mannopyranoside at 37ºC for 2 h. The eluates were then resolved on 3-8% w/v non-denaturing PAGE (Bio-Rad Laboratories Ltd, Hertforshire UK) and immunoblotted for total α_1-antitrypsin.

Immunoprecipitation

For immunoprecipitation (IP), cell lysates or culture media were mixed on the rotator with 1 μg of purified anti-polymer 2C1 mAb [28] for 1 hour at 4ºC. Recombinant protein G agarose beads (ThermoFisher) were then added and the sample incubated on the rotator overnight at 4ºC. The supernatant was collected and subjected to a further 2 rounds of IP with the 2C1 mAb and the residual monomeric species of α_1-antitrypsin were immunoprecipitated with the anti-total α_1-antitrypsin 3C11 mAb [56]. For the experiment shown in Figure 5B, the culture media and cell lysate samples were sequentially immunoprecipitated 4 times with the anti-polymer 2C1 mAb, to ensure that all the polymers had been captured, once with anti-M* intermediate 5E3 mAb [32] and finally with anti-total α_1-antitrypsin 3C11 mAb. At the end of each IP step, beads were collected, washed 3 times with 1% v/v NP-40 buffer and once with 10 mM Tris pH 7.4 and eluted in loading buffer (New England Biolabs Ltd, Hertforshire, UK) in reducing conditions at 93ºC for 5 min. The eluate was then resolved on 4-12% w/v acrylamide SDS PAGE (Bio-Rad Laboratories Ltd, Hertforshire UK) followed by either immunoblotting with polyclonal rabbit anti-α_1-antitrypsin (Dako, Agilent, CA, USA) or autoradiography, as detailed in figure legends.

Cells subjected to treatment with the experimental compound were incubated with 10 μM of the small molecule during the induction with doxycycline. After 48 h induction, cells were washed in pre-warmed PBS and incubated in OptiMEM (Thermo Fisher Scientific Ltd, Loughborough, UK) for 4 h at 37ºC. The culture media containing the experimental compound was changed every 48 h.

Secretion assay and sandwich ELISA

After 48 h induction with 0.5 μg/ml doxycycline, CHO K1 cells were washed twice in pre-warmed PBS and then incubated at 37ºC with OptiMEM (Gibco, Thermo Fisher Scientific Ltd, Loughborough, UK). After a 12 h incubation, culture medium was collected, centrifuged at 300 g for 5 min and 4ºC, transferred into a clean tube and subjected to IP or concentration by ConA-agarose resin. The serum samples from patients were analysed by sandwich ELISA as previously described [28].

Metabolic labelling and pulse-chase

CHO K1 cells were labelled after 48 h induction with 0.5 μg/mL doxycycline and iPSC-derived hepatocytes after differentiation to the hepatocyte stage. Cells were pulsed (0.45MBq/10^6 cells) for 10 min with ^{35}S Cys/Met (EasyTag™ Express Protein Labelling, Perkin Elmer, Beaconsfield, UK) in DMEM without Cys/Met, and then chased in normal culture medium for 0, 0.5, 1, 2, 4, 8 and 12 h. Long metabolic labelling (0.9MBq/10^6 cells) was performed with ^{35}S Cys/Met for 12 h in the presence of cold methionine and cysteine. Cells were then cultured for 12 h in normal medium to promote the incorporation of all the radioactive monomeric α_1-antitrypsin into polymers. After the pulse, cells were chased at 0, 3, 12, 24, 36, 48, 60 and 72 h for CHO K1 cells and up to 108 h for iPSC-derived hepatocytes. Radiolabelled α_1-antitrypsin was isolated by IP and resolved by SDS-PAGE followed by autoradiography. Densitometric analysis of α_1-antitrypsin bands was performed with ImageStudioLite (LI-COR Biosciences, USA). Statistical analysis was performed using the GraphPad Prism program (GraphPad Software, La Jolla, CA, USA).

SDS-PAGE, native PAGE and immunoblot

Material obtained from IP or ConA-agarose concentration as described in the previous section was resolved either by SDS-PAGE or non-denaturing PAGE on pre-cast NuPAGE™ 4-12% w/v acrylamide Bis-Tris Protein Gels and NativePAGE™ 3-12% w/v acrylamide Bis-Tris Protein Gels (Bio-Rad Laboratories Ltd, Hertforshire UK) respectively. Samples were then transferred to LF-PVDF membranes (Millipore Ltd, Hertforshire UK). Membranes were saturated in 5% w/v low-fat milk (Cell Signaling technology, New England Biolabs Ltd, Hertforshire UK) in PBS-0.1% v/v

Tween, probed with the indicated primary antibodies and horseradish peroxidase (HRP)-conjugated secondary antibodies (Santa Cruz Biotechnology, USA), and revealed by ECL (Clarity, Bio-Rad Laboratories Ltd, Hertforshire UK). Western blot images were acquired with the Image Quant Las400 (GE Healthcare Life Sciences, CA, USA) and analysed with Image Studio Lite software (LI-COR Biosciences, Cambridge UK). Statistical analysis was performed using the GraphPad Prism program.

Human plasma samples

All human biological samples were obtained with informed consent under an IRB/EC protocol approved by NRES Committee London-Hampstead (REC Ref. 13/LO/1085, IRAS Project ID 130158, Study Title: Targeting Dysfunctional Mechanisms in α_1-antitrypsin deficiency).

Author Contributions

RR, AP, JI and DL designed research; RR, NHC and JI analysed data; RR, NHC and MR performed the research; RR, AF, EM, JI and DL wrote the paper.

Acknowledgments

This work was supported by GlaxoSmithKline, the Medical Research Council (UK) (grant number MR/NO24842/1) and the NIHR UCLH Biomedical Research Centre. This work was funded in part by a grant from Alpha-1 Foundation (USA) (grant number 615837) to RR. E. Miranda is funded by the Alpha-1 Foundation (USA) and the Pasteur Institute-Cenci Bolognetti Foundation (Italy). D. Lomas is an NIHR Senior Investigator.

References

1 Gooptu B & Lomas DA (2009) Conformational pathology of the serpins: themes, variations, and therapeutic strategies. *Annu Rev Biochem* **78**, 147–176.

2 Lomas DA (2016) Does Protease-Antiprotease Imbalance Explain Chronic Obstructive Pulmonary Disease? *Ann Am Thorac Soc* **13 Suppl 2**, S130-137.

3 Lomas DA, Evans DL, Finch JT & Carrell RW (1992) The mechanism of Z alpha 1-antitrypsin accumulation in the liver. *Nature* **357**, 605–607.

4 Janciauskiene S, Eriksson S, Callea F, Mallya M, Zhou A, Seyama K, Hata S & Lomas DA (2004) Differential detection of PAS-positive inclusions formed by the Z, Siiyama, and Mmalton variants of alpha1-antitrypsin. *Hepatol Baltim Md* **40**, 1203–1210.

5 Granell S, Baldini G, Mohammad S, Nicolin V, Narducci P, Storrie B & Baldini G (2008) Sequestration of mutated alpha1-antitrypsin into inclusion bodies is a cell-protective mechanism to maintain endoplasmic reticulum function. *Mol Biol Cell* **19**, 572–586.

6 Eriksson S, Carlson J & Velez R (1986) Risk of cirrhosis and primary liver cancer in alpha 1-antitrypsin deficiency. *N Engl J Med* **314**, 736–739.

7 Dafforn TR, Mahadeva R, Elliott PR, Sivasothy P & Lomas DA (1999) A kinetic mechanism for the polymerization of alpha1-antitrypsin. *J Biol Chem* **274**, 9548–9555.

8 Gooptu B, Hazes B, Chang WS, Dafforn TR, Carrell RW, Read RJ & Lomas DA (2000) Inactive conformation of the serpin alpha(1)-antichymotrypsin indicates two-stage insertion of the reactive loop: implications for inhibitory function and conformational disease. *Proc Natl Acad Sci U S A* **97**, 67–72.

9 Gooptu B, Ekeowa UI & Lomas DA (2009) Mechanisms of emphysema in alpha1-antitrypsin deficiency: molecular and cellular insights. *Eur Respir J* **34**, 475–488.

10 Nyon MP, Segu L, Cabrita LD, Lévy GR, Kirkpatrick J, Roussel BD, Patschull AOM, Barrett TE, Ekeowa UI, Kerr R, Waudby CA, Kalsheker N, Hill M, Thalassinos K, Lomas DA, Christodoulou J & Gooptu B (2012) Structural dynamics associated with intermediate formation in an archetypal conformational disease. *Struct Lond Engl 1993* **20**, 504–512.

11 Ekeowa UI, Freeke J, Miranda E, Gooptu B, Bush MF, Pérez J, Teckman J, Robinson CV & Lomas DA (2010) Defining the mechanism of polymerization in the serpinopathies. *Proc Natl Acad Sci U S A* **107**, 17146–17151.

12 Yamasaki M, Sendall TJ, Pearce MC, Whisstock JC & Huntington JA (2011) Molecular basis of α1-antitrypsin deficiency revealed by the structure of a domain-swapped trimer. *EMBO Rep* **12**, 1011–1017.

13 Tsutsui Y, Kuri B, Sengupta T & Wintrode PL (2008) The Structural Basis of Serpin Polymerization Studied by Hydrogen/Deuterium Exchange and Mass Spectrometry. *J Biol Chem* **283**, 30804–30811.

14 Dunstone MA & Whisstock JC (2011) Crystallography of Serpins and Serpin Complexes. In *Methods in Enzymology* pp. 63–87. Elsevier.

15 Dunstone MA, Dai W, Whisstock JC, Rossjohn J, Pike RN, Feil SC, Le Bonniec BF, Parker MW & Bottomley SP (2000) Cleaved antitrypsin polymers at atomic resolution. *Protein Sci Publ Protein Soc* **9**, 417–420.

16 Yamasaki M, Li W, Johnson DJD & Huntington JA (2008) Crystal structure of a stable dimer reveals the molecular basis of serpin polymerization. *Nature* **455**, 1255–1258.

17 Hidvegi T, Schmidt BZ, Hale P & Perlmutter DH (2005) Accumulation of mutant alpha1-antitrypsin Z in the endoplasmic reticulum activates caspases-4 and -12, NFkappaB, and BAP31 but not the unfolded protein response. *J Biol Chem* **280**, 39002–39015.

18 Davies MJ & Lomas DA (2008) The molecular aetiology of the serpinopathies. *Int J Biochem Cell Biol* **40**, 1273–1286.

19 Ordóñez A, Snapp EL, Tan L, Miranda E, Marciniak SJ & Lomas DA (2013) Endoplasmic reticulum polymers impair luminal protein mobility and sensitize to cellular stress in alpha1-antitrypsin deficiency. *Hepatol Baltim Md* **57**, 2049–2060.

20 Dickens JA, Ordóñez A, Chambers JE, Beckett AJ, Patel V, Malzer E, Dominicus CS, Bradley J, Peden AA, Prior IA, Lomas DA & Marciniak SJ (2016) The endoplasmic reticulum remains functionally connected by vesicular transport after its fragmentation in cells expressing Z-α1-antitrypsin. *FASEB J Off Publ Fed Am Soc Exp Biol* **30**, 4083–4097.

21 Le A, Ferrell GA, Dishon DS, Le QQ & Sifers RN (1992) Soluble aggregates of the human PiZ alpha 1-antitrypsin variant are degraded within the endoplasmic reticulum by a mechanism sensitive to inhibitors of protein synthesis. *J Biol Chem* **267**, 1072–1080.

22 Kroeger H, Miranda E, MacLeod I, Pérez J, Crowther DC, Marciniak SJ & Lomas DA (2009) Endoplasmic Reticulum-associated Degradation (ERAD) and Autophagy Cooperate to Degrade Polymerogenic Mutant Serpins. *J Biol Chem* **284**, 22793–22802.

23 Teckman JH, Burrows J, Hidvegi T, Schmidt B, Hale PD & Perlmutter DH (2001) The proteasome participates in degradation of mutant alpha 1-antitrypsin Z in the endoplasmic reticulum of hepatoma-derived hepatocytes. *J Biol Chem* **276**, 44865–44872.

24 Wu Y, Swulius MT, Moremen KW & Sifers RN (2003) Elucidation of the molecular logic by which misfolded alpha 1-antitrypsin is preferentially selected for degradation. *Proc Natl Acad Sci U S A* **100**, 8229–8234.

25 Mukherjee A, Hidvegi T, Araya P, Ewing M, Stolz DB & Perlmutter DH (2018) NFκB mitigates the pathological effects of misfolded α1-antitrypsin by activating autophagy and an integrated program of proteostasis mechanisms. *Cell Death Differ* **26**, 455–469.

26 Forrester A, De Leonibus C, Grumati P, Fasana E, Piemontese M, Staiano L, Fregno I, Raimondi A, Marazza A, Bruno G, Iavazzo M, Intartaglia D, Seczynska M, van Anken E, Conte I, De Matteis MA, Dikic I, Molinari M & Settembre C (2018) A selective ER-phagy exerts procollagen quality control via a Calnexin-FAM134B complex. *EMBO J*, e99847.

27 Fregno I & Molinari M (2018) Endoplasmic reticulum turnover: ER-phagy and other flavors in selective and non-selective ER clearance. *F1000Research* **7**, 454.

28 Miranda E, Pérez J, Ekeowa UI, Hadzic N, Kalsheker N, Gooptu B, Portmann B, Belorgey D, Hill M, Chambers S, Teckman J, Alexander GJ, Marciniak SJ & Lomas DA (2010) A novel monoclonal antibody to characterize pathogenic polymers in liver disease associated with alpha1-antitrypsin deficiency. *Hepatol Baltim Md* **52**, 1078–1088.

29 Miranda E, Ferrarotti I, Berardelli R, Laffranchi M, Cerea M, Gangemi F, Haq I, Ottaviani S, Lomas DA, Irving JA & Fra A (2017) The pathological Trento variant of alpha-1-antitrypsin (E75V) shows nonclassical behaviour during polymerization. *FEBS J* **284**, 2110–2126.

30 Tan L, Dickens JA, Demeo DL, Miranda E, Perez J, Rashid ST, Day J, Ordoñez A, Marciniak SJ, Haq I, Barker AF, Campbell EJ, Eden E, McElvaney NG, Rennard SI, Sandhaus RA, Stocks JM, Stoller JK, Strange C, Turino G, Rouhani FN, Brantly M & Lomas DA (2014) Circulating polymers in α1-antitrypsin deficiency. *Eur Respir J* **43**, 1501–1504.

31 Fra A, Cosmi F, Ordoñez A, Berardelli R, Perez J, Guadagno NA, Corda L, Marciniak SJ, Lomas DA & Miranda E (2016) Polymers of Z α1-antitrypsin are secreted in cell models of disease. *Eur Respir J* **47**, 1005–1009.

32 Irving JA, Miranda E, Haq I, Perez J, Kotov VR, Faull SV, Motamedi-Shad N & Lomas DA (2015) An antibody raised against a pathogenic serpin variant induces mutant-like behaviour in the wild-type protein. *Biochem J* **468**, 99–108.

33 Fra AM, Gooptu B, Ferrarotti I, Miranda E, Scabini R, Ronzoni R, Benini F, Corda L, Medicina D, Luisetti M & Schiaffonati L (2012) Three New Alpha1-Antitrypsin Deficiency Variants Help to Define a C-Terminal Region Regulating Conformational Change and Polymerization. *PLoS ONE* **7**, e38405.

34 Ronzoni R, Berardelli R, Medicina D, Sitia R, Gooptu B & Fra AM (2016) Aberrant disulphide bonding contributes to the ER retention of alpha1-antitrypsin deficiency variants. *Hum Mol Genet* **25**, 642–650.

35 Yusa K, Rashid ST, Strick-Marchand H, Varela I, Liu P-Q, Paschon DE, Miranda E, Ordóñez A, Hannan NRF, Rouhani FJ, Darche S, Alexander G, Marciniak SJ, Fusaki N, Hasegawa M, Holmes MC, Di Santo JP, Lomas DA, Bradley A & Vallier L (2011) Targeted gene correction of α1-antitrypsin deficiency in induced pluripotent stem cells. *Nature* **478**, 391–394.

36 Rashid ST, Corbineau S, Hannan N, Marciniak SJ, Miranda E, Alexander G, Huang-Doran I, Griffin J, Ahrlund-Richter L, Skepper J, Semple R, Weber A, Lomas DA & Vallier L (2010) Modeling inherited metabolic disorders of the liver using human induced pluripotent stem cells. *J Clin Invest* **120**, 3127–3136.

37 Wilson AA, Ying L, Liesa M, Segeritz C-P, Mills JA, Shen SS, Jean J, Lonza GC, Liberti DC, Lang AH, Nazaire J, Gower AC, Müeller F-J, Mehta P, Ordóñez A, Lomas DA, Vallier L, Murphy GJ, Mostoslavsky G, Spira A, Shirihai OS, Ramirez MI, Gadue P & Kotton DN

(2015) Emergence of a stage-dependent human liver disease signature with directed differentiation of alpha-1 antitrypsin-deficient iPS cells. *Stem Cell Rep* **4**, 873–885.

38 Sharp LK, Mallya M, Kinghorn KJ, Wang Z, Crowther DC, Huntington JA, Belorgey D & Lomas DA (2006) Sugar and alcohol molecules provide a therapeutic strategy for the serpinopathies that cause dementia and cirrhosis. *FEBS J* **273**, 2540–2552.

39 Jeppsson JO, Laurell CB, Nosslin B & Cox DW (1978) Catabolic rate of alpha1-antitrypsin of of Pi types S, and MMalton and of asialylated M-protein in man. *Clin Sci Mol Med* **55**, 103–107.

40 Lamriben L, Oster ME, Tamura T, Tian W, Yang Z, Clausen H & Hebert DN (2018) EDEM1's mannosidase-like domain binds ERAD client proteins in a redox-sensitive manner and possesses catalytic activity. *J Biol Chem* **293**, 13932–13945.

41 Khodayari N, Marek G, Lu Y, Krotova K, Wang RL & Brantly M (2017) Erdj3 Has an Essential Role for Z Variant Alpha-1-Antitrypsin Degradation. *J Cell Biochem* **118**, 3090–3101.

42 Feng L, Zhang J, Zhu N, Ding Q, Zhang X, Yu J, Qiang W, Zhang Z, Ma Y, Huang D, Shen Y, Fang S, Yu Y, Wang H & Shen Y (2017) Ubiquitin ligase SYVN1/HRD1 facilitates degradation of the SERPINA1 Z variant/α-1-antitrypsin Z variant via SQSTM1/p62-dependent selective autophagy. *Autophagy* **13**, 686–702.

43 Tang Y, Blomenkamp KS, Fickert P, Trauner M & Teckman JH (2018) NorUDCA promotes degradation of α1-antitrypsin mutant Z protein by inducing autophagy through AMPK/ULK1 pathway. *PloS One* **13**, e0200897.

44 Lomas DA, Irving JA, Arico-Muendel C, Belyanskaya S, Brewster A, Brown M, Chung C, Dave H, Denis A, Dodic N, Dossang A, Eddershaw P, Klimaszewska D, Haq I, Holmes DS, Hutchinson JP, Jagger A, Jakhria T, Jigorel E, Liddle J, Lind K, Marciniak SJ, Messer J, Neu M, Olszewski A, Ordonez A, Ronzoni R, Rowedder J, Rüdiger M, Skinner S, Smith KJ, Terry R, Trottet L, Uings I, Wilson S, Zhu Z & Pearce AC (2020) *Development of a small molecule that corrects misfolding and increases secretion of Z* α_1 *-antitrypsin* Pharmacology and Toxicology. BioRxiv.

45 Powell LM & Pain RH (1992) Effects of glycosylation on the folding and stability of human, recombinant and cleaved alpha 1-antitrypsin. *J Mol Biol* **224**, 241–252.

46 James EL, Whisstock JC, Gore MG & Bottomley SP (1999) Probing the unfolding pathway of alpha1-antitrypsin. *J Biol Chem* **274**, 9482–9488.

47 Yu MH, Lee KN & Kim J (1995) The Z type variation of human alpha 1-antitrypsin causes a protein folding defect. *Nat Struct Biol* **2**, 363–367.

48 Haq I, Irving JA, Faull SV, Dickens JA, Ordóñez A, Belorgey D, Gooptu B & Lomas DA (2013) Reactive centre loop mutants of α-1-antitrypsin reveal position-specific effects on intermediate formation along the polymerization pathway. *Biosci Rep* **33**.

49 Knaupp AS, Levina V, Robertson AL, Pearce MC & Bottomley SP (2010) Kinetic instability of the serpin Z alpha1-antitrypsin promotes aggregation. *J Mol Biol* **396**, 375–383.

50 Ekeowa UI, Freeke J, Miranda E, Gooptu B, Bush MF, Pérez J, Teckman J, Robinson CV & Lomas DA (2010) Defining the mechanism of polymerization in the serpinopathies. *Proc Natl Acad Sci U S A* **107**, 17146–17151.

51 Blomenkamp KS & Teckman JH (2017) Semiquantitation of Monomer and Polymer Alpha-1 Antitrypsin by Centrifugal Separation and Assay by Western Blot of Soluble and Insoluble Components. In *Alpha-1 Antitrypsin Deficiency* (Borel F & Mueller C, eds), pp. 227–234. Springer New York, New York, NY.

52 Anelli T & Sitia R (2008) Protein quality control in the early secretory pathway. *EMBO J* **27**, 315–327.

53 Helenius A & Aebi M (2004) Roles of N-Linked Glycans in the Endoplasmic Reticulum. *Annu Rev Biochem* **73**, 1019–1049.

54 Wang Y, Cobanoglu MC, Li J, Hidvegi T, Hale P, Ewing M, Chu AS, Gong Z, Muzumdar R, Pak SC, Silverman GA, Bahar I & Perlmutter DH (2019) An analog of glibenclamide selectively enhances autophagic degradation of misfolded α1-antitrypsin Z. *PloS One* **14**, e0209748.

55 Teckman JH, An J-K, Loethen S & Perlmutter DH (2002) Fasting in alpha1-antitrypsin deficient liver: constitutive [correction of consultative] activation of autophagy. *Am J Physiol Gastrointest Liver Physiol* **283**, G1156-1165.

56 Tan L, Perez J, Mela M, Miranda E, Burling KA, Rouhani FN, DeMeo DL, Haq I, Irving JA, Ordóñez A, Dickens JA, Brantly M, Marciniak SJ, Alexander GJM, Gooptu B & Lomas DA

(2015) Characterising the association of latency with α(1)-antitrypsin polymerisation using a novel monoclonal antibody. *Int J Biochem Cell Biol* **58**, 81–91.

57 Irving JA, Ekeowa UI, Belorgey D, Haq I, Gooptu B, Miranda E, Pérez J, Roussel BD, Ordóñez A, Dalton LE, Thomas SE, Marciniak SJ, Parfrey H, Chilvers ER, Teckman JH, Alam S, Mahadeva R, Rashid ST, Vallier L & Lomas DA (2011) Chapter Eighteen - The Serpinopathies: Studying Serpin Polymerization In Vivo. In *Methods in Enzymology* (Whisstock JC & Bird PI, eds), pp. 421–466. Academic Press.

mAb	*mAb specificity*	*references*
2C1	α1-antitrypsin polymers	Miranda et al.; 2010 [28]
3C11	total α1-antitrypsin	Tan et al.; 2014 [30]
5E3	α1-antitrypsin folding intermediate (M*)	Irving et al.; 2015 [32]

Table 1

Title: mAbs specificity

Table 2

Title: Soluble and insoluble polymers half-life

		Half-life (h)	*Std error*	*n of indep. exps.*	*Df* [a]
CHO K1 AAT Z	Soluble Polymers	10.9	1.7	7	47
	Insoluble Polymers	20.9	7.4	2	13
iPSCs-derived hepatocytes					
	Soluble Polymers	14.7	6.2	5	29
	Insoluble Polymers	19.1	4.9	2	9

Figure legends

Figure 1. Identification of polymers in the soluble and insoluble intracellular fractions of cells expressing Z α_1-antitrypsin. (A) CHO inducible cells expressing either M or Z α_1-antitrypsin were induced with 0.5 μg/mL doxycycline for 48 h and then lysed in 1% v/v NP-40 buffer. The soluble (Sol), insoluble (Insol) and extracellular (EC) fractions were separated by 4-12% w/v acrylamide SDS-PAGE and the proteins visualised by immunoblotting for total α_1-antitrypsin with the 3C11 mAb. White and black arrowheads indicate the mature and immature glycosylated forms of α_1-antitrypsin respectively. The percentage of intracellular and secreted α_1-antitrypsin was calculated by densitometric quantification. Graph shows mean ± standard error of the mean (±SEM, n=3). (B) Cell lysates from CHO cells expressing either M or Z α_1-antitrypsin (as indicated) were concentrated with ConA beads and eluted as described in Methods. The samples were then resolved on a 3-12% w/v acrylamide non-denaturing gel followed by immunoblotting for total α_1-antitrypsin. White and black arrowheads indicate the mature and immature glycosylated forms of α_1-antitrypsin respectively. The different charges acquired from the glycosylation process make the mature form of the protein run faster than the immature form. Monomeric secreted Z α_1-antitrypsin in the supernatant migrates more slowly in non-denaturing PAGE than secreted M α_1-antitrypsin as a result of the Glu342Lys mutation. The immunoblot is representative of 3 independent experiments. (C) 1% v/v NP-40 soluble and insoluble fractions from cells expressing either M or Z α_1-antitrypsin were sequentially immunoprecipitated using the 2C1 polymer-specific mAb (3 times) and the 3C11 mAb against total α_1-antitrypsin (once) as indicated for Set 1. The fractions were also immunoprecipitated 3 times with the 3C11 mAb and once with 2C1 mAb as shown in Set 2. Proteins were eluted with an SDS-based buffer and analysed by 4-12% w/v acrylamide SDS PAGE followed by immunoblotting for α_1-antitrypsin with polyclonal antibody. Western blots are representative of 2 independent experiments.

Figure 2. Kinetics of intracellular accumulation and secretion of Z α_1-antitrypsin polymers. (A) CHO-K1 Tet-On cells expressing either M or Z α_1-antitrypsin were induced with doxycycline for 48 h. Cells were labelled for 10 minutes with ^{35}S Met/Cys and chased at the indicated times. Culture

media were collected and cells lysed in 1% v/v NP-40 buffer. Intracellular fractions and culture media from cells expressing Z α_1-antitrypsin were immunoprecipitated twice with the polymer-specifc mAb (2C1) and then with a mAb against total α_1-antitrypsin (3C11). Samples were resolved by 4-12% w/v acrylamide SDS-PAGE and detected by autoradiography. White and black arrowheads indicate the mature and immature glycosylated forms of α_1-antitrypsin respectively. Autoradiograms are representative of 3 independent experiments. (B) Densitometric analysis of the bands in Fig. 2A. Graph shows mean ± standard error of the mean (±SEM, n=3). Densitometry of the bands was analysed by ImageStudio software. Dotted lines are only intended to indicate the trend of the data. (C) The media from the cell culture expressing Z α_1-antitrypsin, shown in panel A, were treated with either endoglycosidase H (H) or peptide-N-glycosidase F (F) or not treated (-). Samples were then analysed by SDS-PAGE and detected by autoradiography. Black and white arrowheads indicate the glycosylated and deglycosylated forms of α_1-antitrypsin respectively. (D) CHO-K1 Tet-On cells expressing Z α_1-antitrypsin were induced with doxycycline for 48 h, labelled for 12 h with ^{35}S Met/Cys and then incubated for 12 h with normal medium with 0.5 μg/mL doxycycline. Culture media were collected at the specific chase time points and cells lysed in 1% v/v NP-40 buffer. The intracellular fractions were immunoprecipitated with the 2C1 polymer-specific mAb, samples were separated on a 4-12% w/v acrylamide SDS-PAGE and detected by autoradiography. Graph shows mean ± standard deviation (soluble polymers ±SD, n=7, insoluble polymers ±SD, n=2). Densitometry of the bands was analysed by ImageStudio software. The gels are representative of the experiments reported in Table 2.

Figure 3. Extracellular polymers are not formed post-secretion. (A) Plasma samples from 3 different Pi ZZ α_1-antitrypsin individuals were heated for 24 h at 20, 37, 41, 45 and 50ºC and subsequently analysed by sandwich ELISA, using the 3C11 mAb (total α_1-antitrypsin) or 2C1 mAb (α_1-antitrypsin polymers) as capture antibodies and a polyclonal antibody HRP-conjugated for detection. The graphs show mean ± standard error of the amount estimated relative to the respective standard curves (±SEM, n=3) (one-way ANOVA, Bonferroni multiple comparisons test, df=34). (B) The same plasma samples were incubated at 37ºC for 1, 3 and 10 days, and subsequently analysed by the same sandwich ELISA. The graphs show mean ± standard error (±SEM, n=3) (One-way ANOVA,

Bonferroni multiple comparisons test, df=8). Statistical analyses were performed using Graph Pad Prism.

Figure 4. Inhibition of the proteasome increases soluble intracellular Z α_1-antitrypsin polymers. (A) CHO-K1 Tet-On cells expressing Z α_1-antitrypsin were induced with doxycycline for 48 h, treated with 80 μM MG132, labelled for 10 minutes with ^{35}S Met/Cys and chased at the reported times. Culture media were collected and cells lysed in 1% v/v NP-40 buffer. Intracellular fractions and culture media were immunoprecipitated twice with the polymer-specific mAb 2C1 and then with the 3C11 mAb against total α_1-antitrypsin. Samples were resolved by 4-12% w/v acrylamide SDS-PAGE and detected by autoradiography. White and black arrowheads indicate the mature and immature glycosylated forms of α_1-antitrypsin respectively. Representative of 3 independent experiments. (B) Graphs show densitometric analysis of MG132 pulse chase experiments in Fig. 4A (mean ± SEM, n=3). Densitometry of the bands was performed by Image Studio software. Statistical analysis (2-way ANOVA) was calculated using GraphPad Prism. Dotted lines are intended to indicate the trend of the data only. Protein precipitated in the first round of immunoprecipitation with the 2C1 mAb is denoted 'polymer'. 'Monomer' refers to residual α_1-antitrypsin immunoprecipitated by the 3C11 mAb after 2 rounds of immunoprecipitation with the 2C1 mAb. (C) CHO cells expressing Z α_1-antitrypsin were induced with 0.5 μg/mL doxycycline and treated with either 50 nM Bafilomycin A1 (BafA1) or 0.1% v/v DMSO (NT) for 16 h. After lysis at the indicated times, 1% v/v NP-40-soluble and -insoluble fractions were separated and sequentially immunoprecipitated with the 2C1 anti-polymer mAb and once with the 3C11 mAb that detects all conformers of α_1-antitrypsin. The eluted samples were resolved on 4%-12% w/v acrylamide SDS-PAGE followed by immunoblotting for total α_1-antitrypsin. The top panel is representative of 3 independent experiments and the graph shows mean ± standard error of the mean (±SEM, n=3). Densitometry of the bands was performed by Image Studio software. 'Polymer' denotes the protein precipitated in the first round of immunoprecipitation with the 2C1 mAb. 'Monomer' refers to residual α_1-antitrypsin immunoprecipitated by the 3C11 mAb after 2 rounds of immunoprecipitation with the 2C1 mAb.

Figure 5. Detection of the folding intermediate M* in cells. (A) CHO-K1 Tet-On cells expressing Z α_1-antitrypsin were induced with doxycycline and treated either with the small molecule polymerisation inhibitor (c716) or with 0.1% v/v DMSO for 48 h and labelled for 10 minutes with ^{35}S Met/Cys. Culture media were collected and cells lysed in 1% v/v NP-40 buffer as described above. Intracellular fractions and cell media were immunoprecipitated with the 2C1 anti-polymer mAb and then the 3C11 total α_1-antitrypsin mAb. Samples were resolved by 4%-12% w/v acrylamide SDS-PAGE and the proteins detected by autoradiography. Densitometry of the bands was performed using Image Studio software. 'Polymer' indicates the protein precipitated in the first round of immunoprecipitation with the 2C1 mAb. 'Monomer' refers to residual α_1-antitrypsin immunoprecipitated by the 3C11 mAb after 2 rounds of immunoprecipitation with the 2C1 mAb. NT represents the densitometric analysis of untreated cells while 'polymer inhibitor' refers to cells treated with the experimental small molecule (c716). The top panels are representative of 2 independent experiments and the graphs show mean ± standard deviation (±SD, n=2). Dotted lines do not show the fit but indicate the trend of the data. (B) CHO cells expressing Z α_1-antitrypsin were induced with 0.5 μg/mL doxycycline and treated with either the small molecule inhibitor of polymerisation (c716) or 0.1% v/v DMSO for 48 h. Cells treated with proteasome inhibitor were incubated with 80 μM MG132 one hour before the beginning of the secretion assay. After washing and incubation in OptiMEM the NP-40 soluble and extracellular fractions were separated and sequentially immunoprecipitated 4 times with the 2C1 anti-polymer mAb, once with the 5E3 anti-M* mAb, and once with the 3C11 mAb that detects all conformers of α_1-antitrypsin. The eluted samples were resolved on 4%-12% w/v acrylamide SDS-PAGE followed by immunoblotting with a rabbit polyclonal anti-α_1-antitrypsin (only the first 2C1 immunoprecipitation is shown). The top panels are representative of 2 independent experiments and the graphs show mean ± standard deviation (±SD, n=2). Asterisk (*) indicates signals from intracellular material released by dead cells. Dotted lines do not show the fit but indicate the trend of the data.

Fig.1

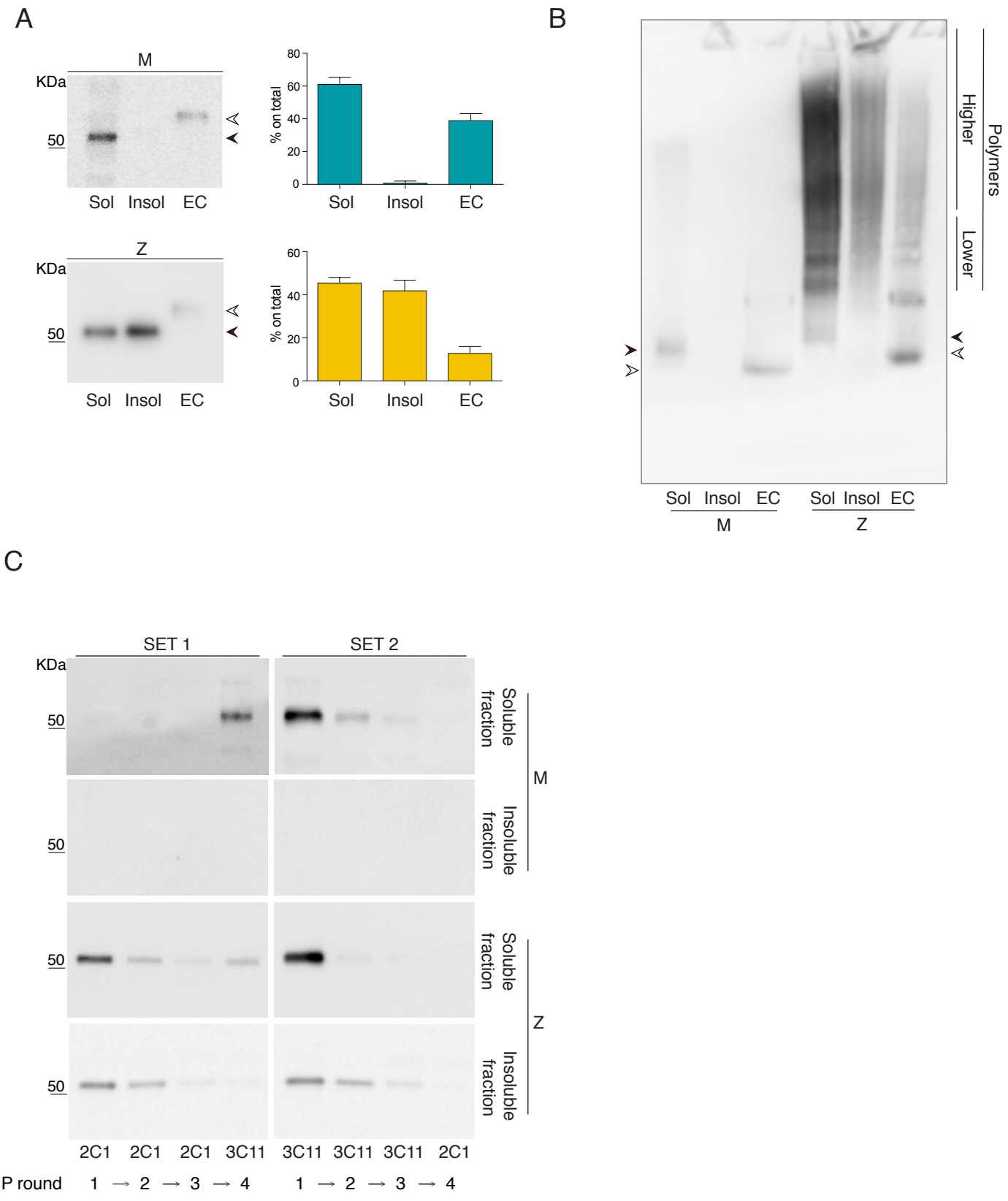
A
M
KDa
50
Sol Insol EC
% on total
80
60
40
20
0
Sol Insol EC
Z
KDa
50
Sol Insol EC
% on total
60
40
20
0
Sol Insol EC
B
Polymers
Higher
Lower
Sol Insol EC Sol Insol EC
M
Z
C
SET 1
SET 2
KDa
50
Soluble fraction
Insoluble fraction
M
Z
2C1 2C1 2C1 3C11 3C11 3C11 3C11 2C1
IP round 1 → 2 → 3 → 4 1 → 2 → 3 → 4

Fig.2

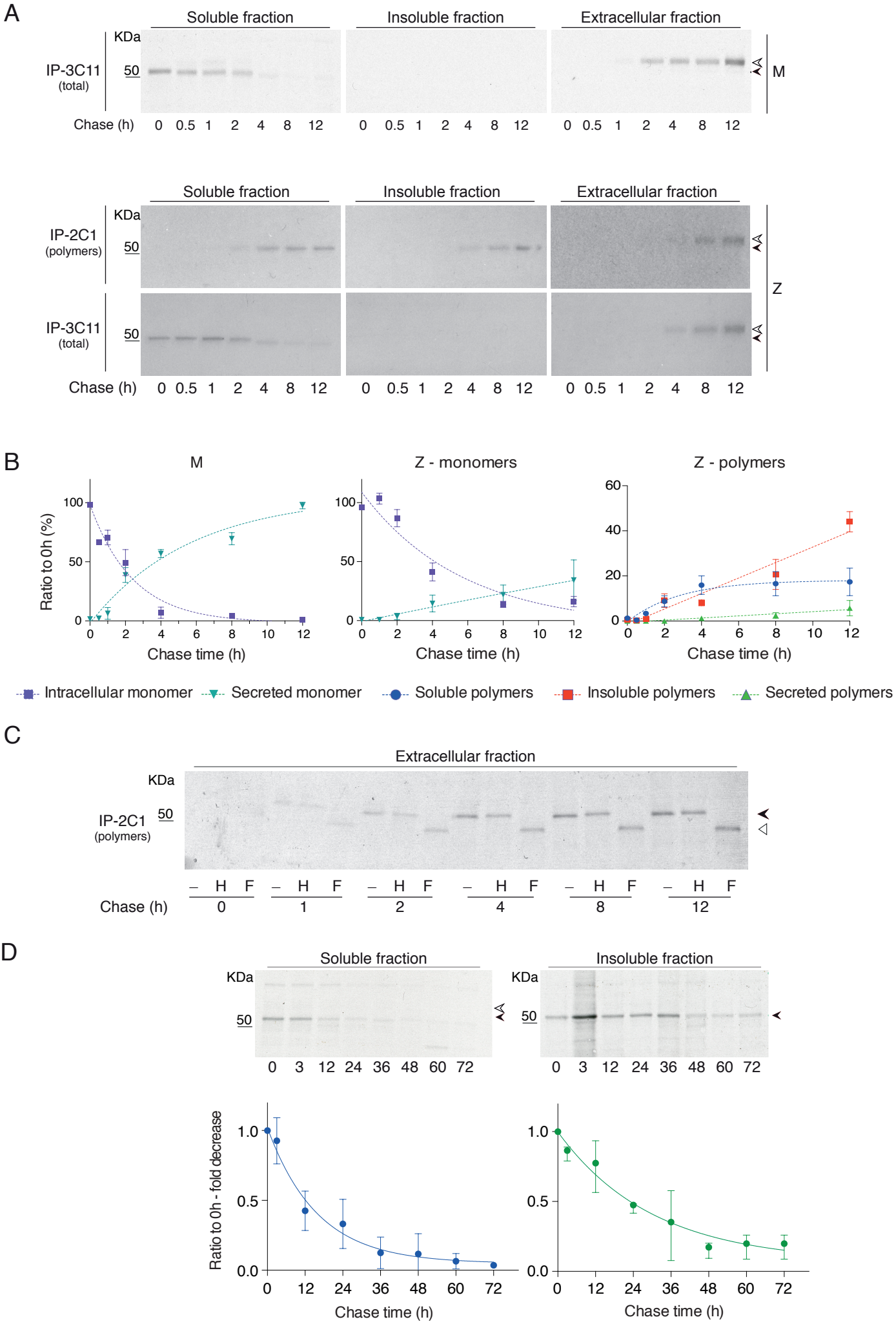
A
Soluble fraction
Insoluble fraction
Extracellular fraction
KDa
IP-3C11
(total)
50
M
Chase (h) 0 0.5 1 2 4 8 12
IP-2C1
(polymers)
Z
B
M
Z - monomers
Z - polymers
Ratio to 0h (%)
Chase time (h)
Intracellular monomer
Secreted monomer
Soluble polymers
Insoluble polymers
Secreted polymers
C
Extracellular fraction
– H F
0 1 2 4 8 12
D
Soluble fraction
Insoluble fraction
0 3 12 24 36 48 60 72
Ratio to 0h - fold decrease

Fig.3

A

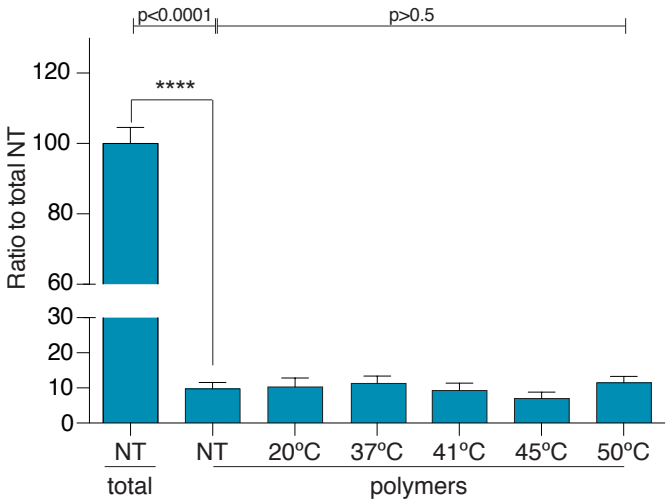
p<0.0001
p>0.5
****
Ratio to total NT
120
100
80
60
30
20
10
0
NT
total
NT
20°C
37°C
41°C
45°C
50°C
polymers

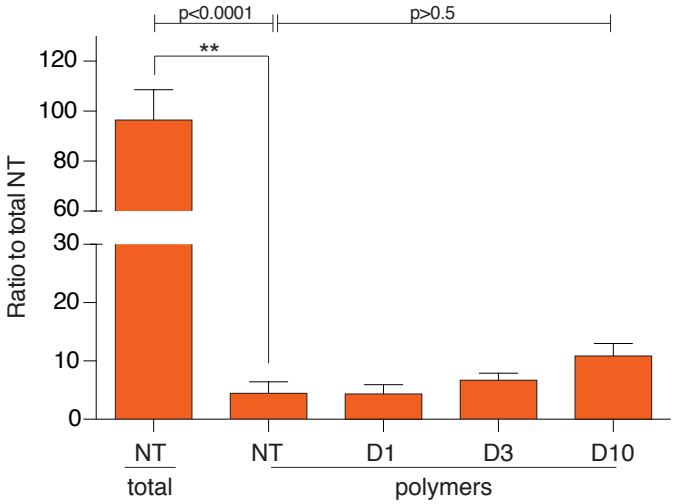
p<0.0001
p>0.5
**
Ratio to total NT
120
100
80
60
30
20
10
0
NT
total
NT
D1
D3
D10
polymers

Fig.4

A

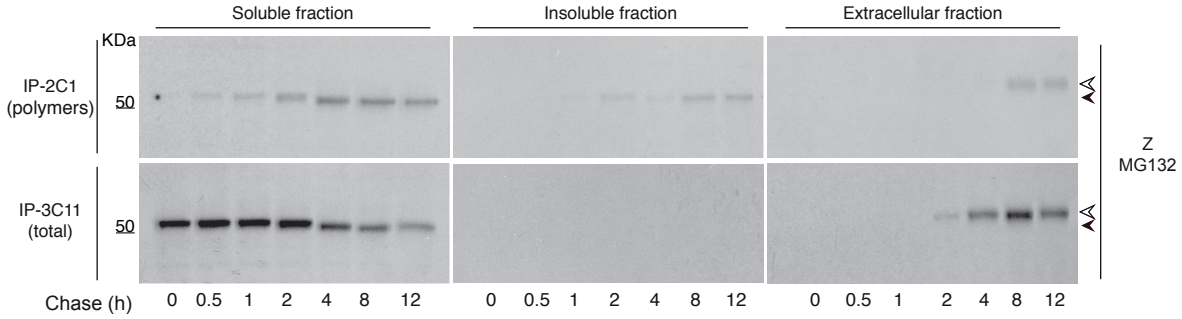
Soluble fraction
Insoluble fraction
Extracellular fraction
KDa
IP-2C1 (polymers)
50
IP-3C11 (total)
50
Z MG132
Chase (h)
0 0.5 1 2 4 8 12

B

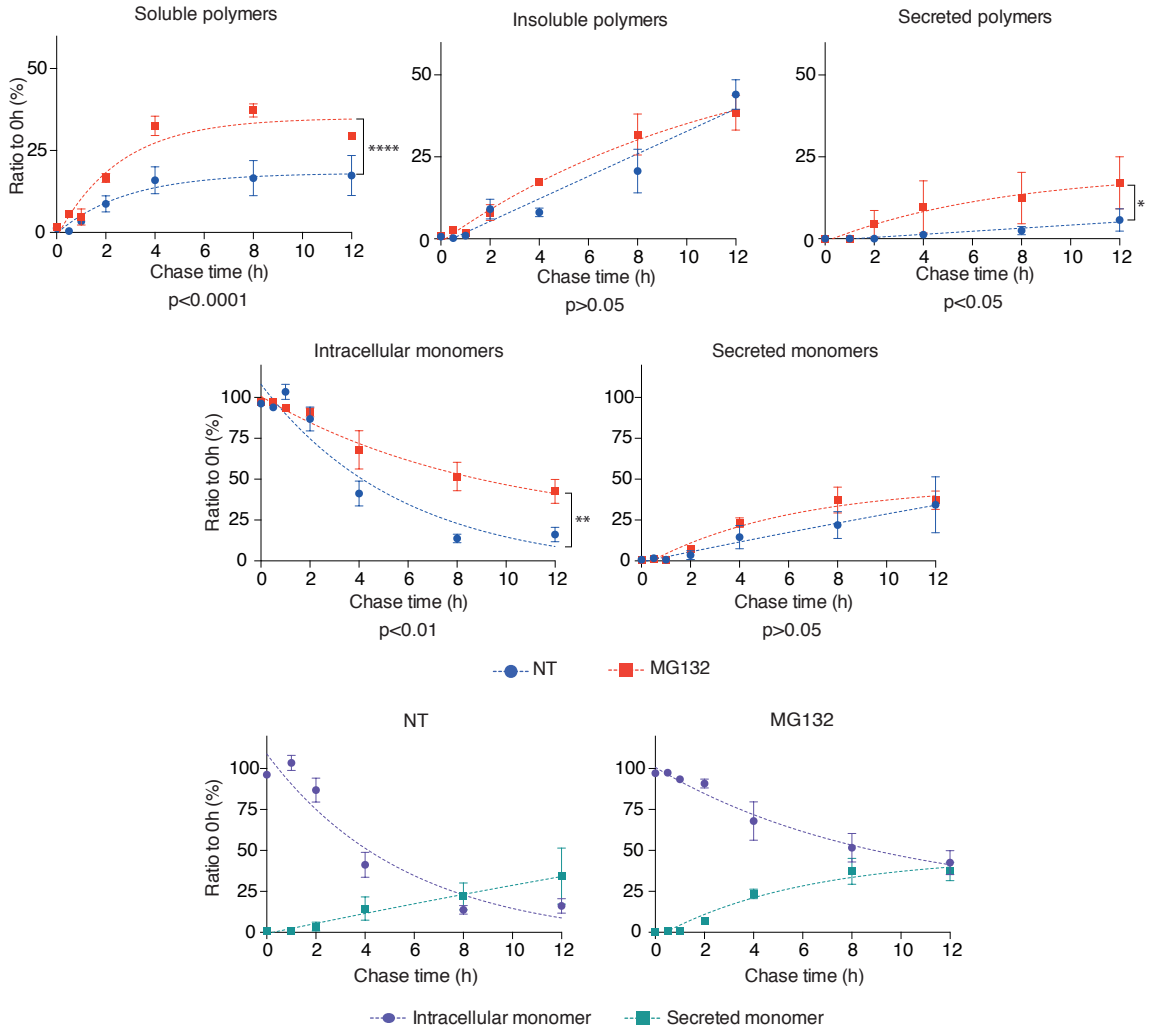
Soluble polymers
Ratio to 0h (%)
Chase time (h)
p<0.0001
Insoluble polymers
p>0.05
Secreted polymers
p<0.05
Intracellular monomers
p<0.01
Secreted monomers
p>0.05
NT
MG132
Intracellular monomer
Secreted monomer

C

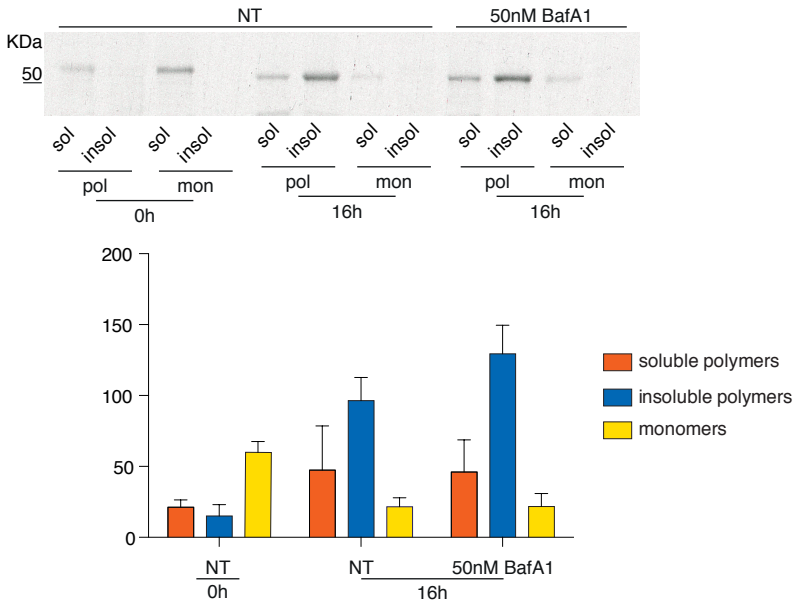
NT
50nM BafA1
KDa
50
sol
insol
pol
mon
0h
16h
soluble polymers
insoluble polymers
monomers

Fig.5

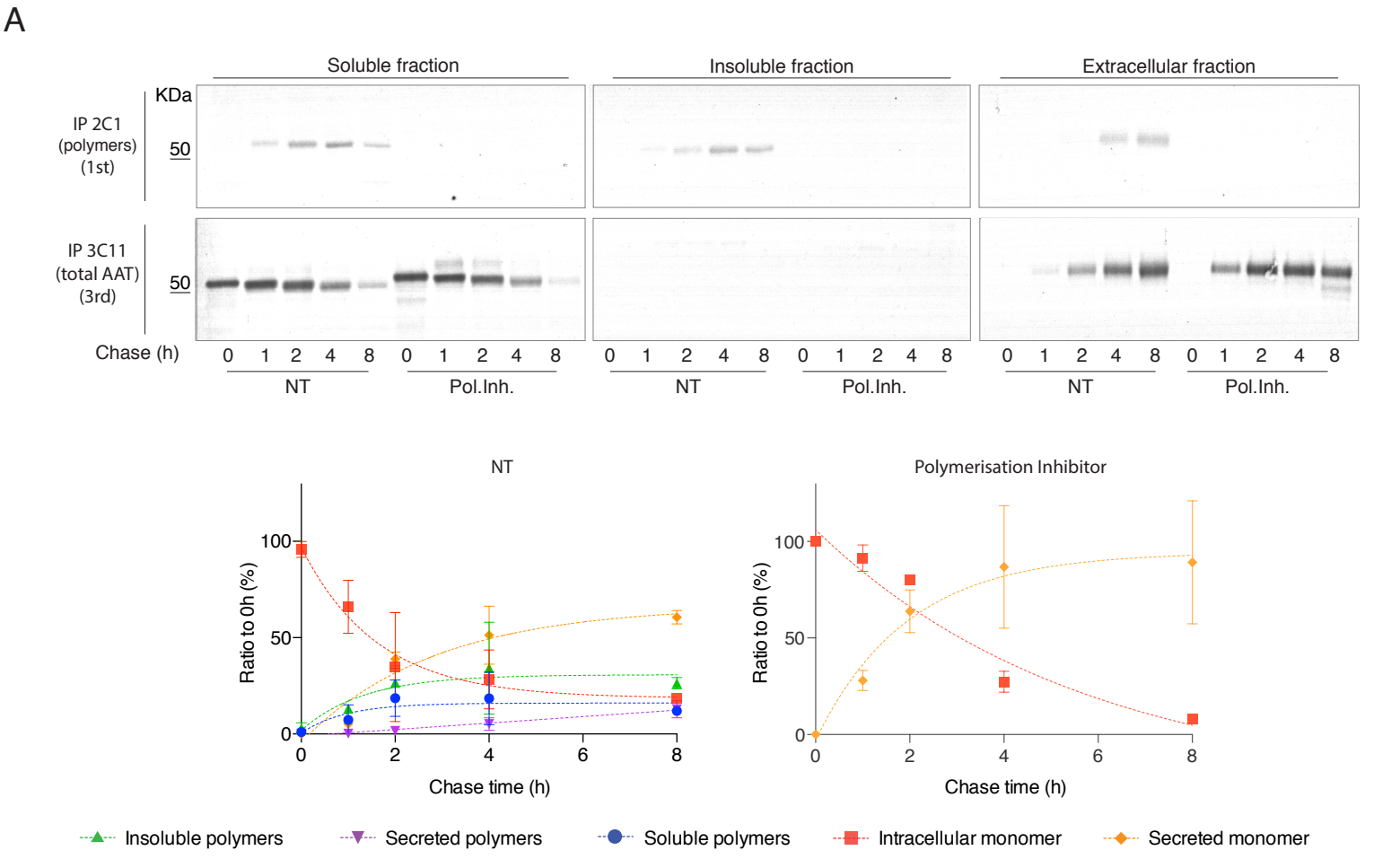
A
Soluble fraction
Insoluble fraction
Extracellular fraction
KDa
IP 2C1 (polymers) (1st)
IP 3C11 (total AAT) (3rd)
50
Chase (h)
0 1 2 4 8 0 1 2 4 8
NT
Pol.Inh.
NT
Polymerisation Inhibitor
Ratio to 0h (%)
Chase time (h)
Insoluble polymers
Secreted polymers
Soluble polymers
Intracellular monomer
Secreted monomer

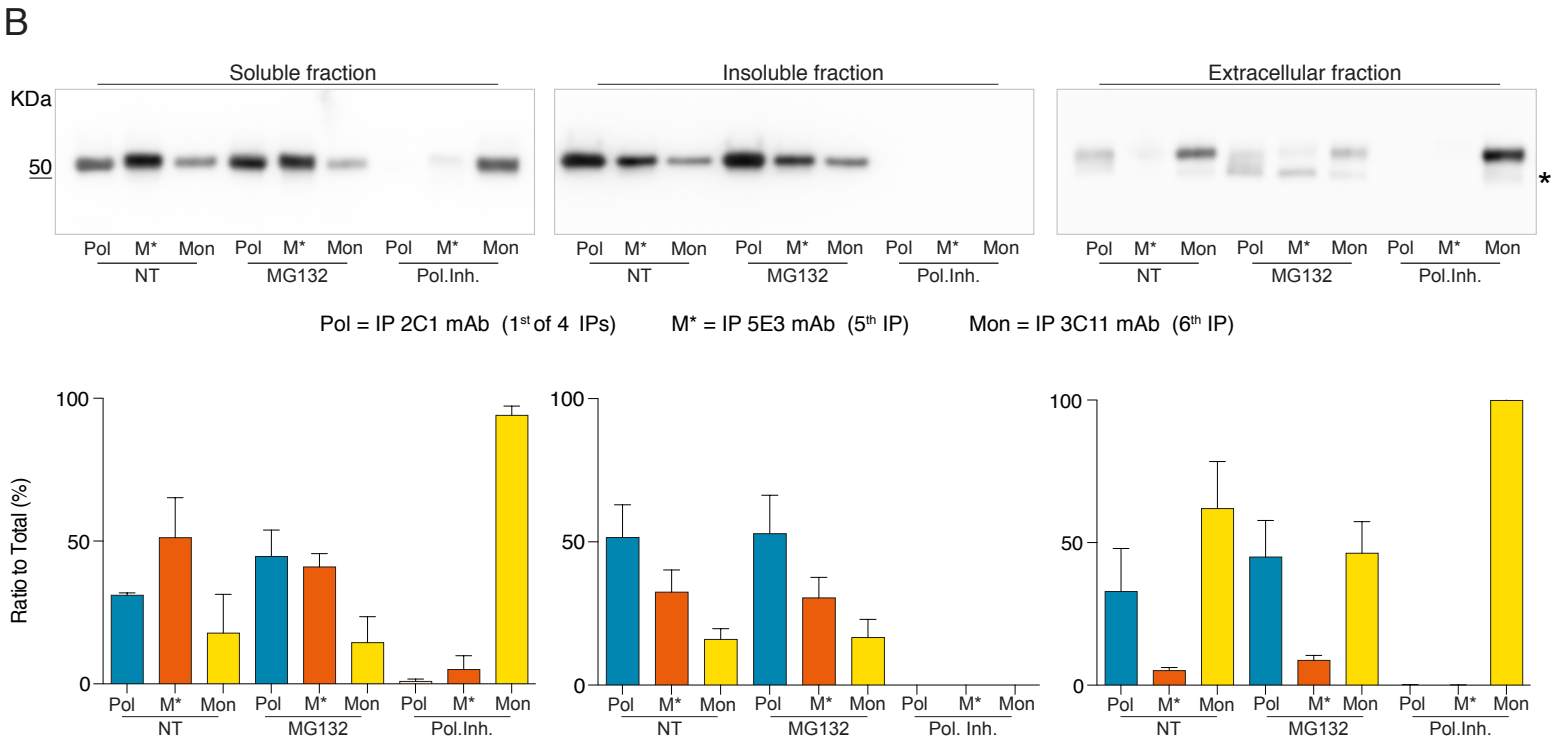
B
Soluble fraction
Insoluble fraction
Extracellular fraction
KDa
50
*
Pol M* Mon
NT
MG132
Pol.Inh.
Pol = IP 2C1 mAb (1st of 4 IPs)
M* = IP 5E3 mAb (5th IP)
Mon = IP 3C11 mAb (6th IP)
Ratio to Total (%)
Pol. Inh.